Identification of the electronic structure differences between polar isostructural FeO and CoO films by core-level soft x-ray spectroscopy

Sarp Kaya, Toyli Anniyev, Hirohito Ogasawara, and Anders Nilsson

Identification of the electronic structure differences between polar isostructural FeO and CoO films by core level soft X-ray spectroscopy

Sarp Kaya,*[1,2] Toyli Anniyev,[3,4] Hirohito Ogasawara,[2] and Anders Nilsson[1,2,3]

[1]SUNCAT Center for Interface Science and Catalysis, SLAC National Accelerator Laboratory, 2575 Sand Hill Rd., Menlo Park, CA 94025, USA

[2]Stanford Synchrotron Radiation Lightsource, SLAC National Accelerator Laboratory, 2575 Sand Hill Rd., Menlo Park, CA 94025, USA

[3]Stanford Institute for Materials and Energy Sciences, SLAC National Accelerator Laboratory, 2575 Sand Hill Rd., Menlo Park, CA 94025, USA

[4]Department of Physics, Stanford University, Stanford, CA 94305, USA

The electronic properties of the FeO and CoO single layer thin films on Pt(111) were examined by core level soft X-ray spectroscopy. These oxygen terminated films are bilayer-thick and isostructural, Pt, Fe-Co, and O atoms stacked with small lateral shifts due to incommensurate relation with Pt(111). Probing occupied and unoccupied states projected on the oxygen atoms revealed states at the Fermi level suggesting orbital mixing with the metal substrate and also indicated an anisotropy in transition metal-oxygen bonding geometry. The differences in the core level spectral features were attributed to the substrate induced modification of the charge transfer energy and with an additional valence electron on Co.

* corresponding author:

Dr. Sarp Kaya

SUNCAT Center for Interface Science and Catalysis

SLAC National Accelerator Laboratory

2575 Sand Hill Rd. Menlo Park, CA 94025, USA

e-mail: sarpkaya@slac.stanford.edu

phone: +1 (650) 926 2011

Introduction

The late transition metal (TM) monoxides are of great interest owing to their importance in catalysis, mineralogy, and device electronics. Particularly, the nature of the (111) terminations is characterized with the polarity that they possess. The alternating layers of $3d$ TM and oxygen atoms accumulating polarity perpendicular to the surface play an important role in material properties but also create stability problems. The free energy requirements of the polar system force the surfaces to compensate the charge built-up by structural and electronic modifications. The compensation channels include (i) the surface reconstructions involving charge redistribution, (ii) anion-cation vacancy generation leading to changes in surface stoichiometry, and (iii) adsorption of foreign species[1]. Theoretical treatments are also challenging, since correlated electron systems make simple approaches fail for estimating standard electronic properties.[2,3] Interestingly, thin films with uncompensated polarity have been found stable if their thickness is below a critical value,[4] there are however deviations from the bulk values in terms of interatomic distances and electronic band gaps.

FeO and CoO are within the $3d$ TM monoxide family, whose ground state electronic configurations for Fe^{2+} and Co^{2+} are d^6 and d^7, respectively. They have been classified as charge transfer insulators in the Zaanen-Sawatzky-Allen phase diagram[5], since the band gaps of the late TM monoxide compounds are found to be smaller than a Mott insulator could have[6]. Recent reports show that the band gaps of the bulk FeO and CoO are 2.4 eV[7] and 2.6 eV[8], respectively. This is also contrary to the classical band theory estimations which dictate that the $3d$ TM monoxides with unfilled $3d$ states must be metallic. Hubbard theory describes this controversy by introducing the d-d Coulomb interaction energy (U_{dd}). However, it is not fully successful to give a full electronic structure picture, especially of the late TMs. Better agreements (based on Anderson impurity model) have been achieved by introduction of the charge transfer energy (Δ), the energy required for transferring a charge from the oxygen ligand to the metal $3d$ states and by including the hybridization strength (T) between O $2p$ ligand and TM $3d$ states. These Coulomb electron correlation and ligand charge fluctuations have generally been denoted by $d^n d^n \rightarrow d^{n-1} d^{n+1}$ and $d^n, \rightarrow d^{n+1}\underline{L}$, respectively; where $\underline{L}$ is a hole in the oxygen ligand. The values of U and Δ relative to the bandwidths of the TM $3d$ (w) and O $2p$ (W) valence states determine if the electronic structure of the TM complex is a conductor, Mott or charge transfer insulator type[5,9].

Thin oxide films grown on metallic substrates have brought a unique concept for studies using surface science techniques utilizing primarily the analysis of low energy electrons since the charging issues can be circumvented[10]. The attractiveness of these systems owing to the resemblance of bulk materials in terms of electronic and geometric structures has been balanced with the discussion regarding the influence of the substrate to those properties[10]. The electronic structures modified by hybridizations with the substrates might deviate from the bulk however it has also been considered to be a design parameter of catalytic systems with superior performance[11]. In the present study our main interest is on the electronic structure of FeO and CoO thin films, which have been grown on several substrates. Early successful attempts include Mo(100)[12], Fe(110)[13], and Cu(110)[14] for FeO and Co(0001)[15], Au(111)[16], and Ir(100)[17] for CoO films. Among these Pt(111) is the unique substrate on which both films can be grown epitaxially with minor structural differences.

The structural characterizations of FeO(111) and CoO(111) epitaxial thin films grown on Pt(111) substrates have been performed in detail. Both TM monoxide films are single TM-O bilayer-thick and oxygen terminated, the metal atoms decorate the interface layer with the same periodicity. The findings of earlier photoelectron diffraction (PD)[18], low energy electron diffraction (LEED), and scanning tunneling microscopy (STM)[19] studies mostly agree with the recent ones[20], that the FeO films grown on Pt(111) have a lattice mismatch which is revealed as a superstructure (Moiré patterns). X-ray photoelectron spectroscopy (XPS) studies show that the oxidation state of Fe is 2+; indicating the formal charges are close to the charges in FeO stoichiometry[21,22]. CoO grows on Pt(111) similarly[23], with the Co possessing formal charges close to those in bulk CoO[24] but much less is known about the electronic structure of this film.

As an alternative to the electronic structure understanding based on bulk materials, these films can also be viewed as oxygen atoms chemisorbed on three-fold sites of $3d$ TM monolayer films. The d-band model[25,26] which correlates the width and the energy position of the valence electron states with the adsorbate states could in principle be adapted to describe the electronic structure and the bonding between TM and O atoms. The latter approach deals with the covalency of the chemical bond thus the strength of the hybridization between TM and oxygen valence states determines the electronic structure of the films. The nature of the chemical bonding between TM and O atoms can thus be defined by bonding and antibonding states of oxygen atoms. It is not clear if the electronic structures of these films are analogous to the bulk

properties which are described by a small band gap. Moreover, polarity is associated with Coulomb repulsion and band filling[27], the anisotropy in TM-O bond distances and orbital symmetry are the factors defining overall stability of these films. Core level (CL) X-ray spectroscopy sheds light on the electronic properties since valence band (VB) and bonding configurations could be probed selectively on various atomic sites.

In this paper, we report on the differences in the electronic structures of FeO and CoO isostructural films grown on a Pt(111) substrate. We adopt CL spectroscopy techniques (X-ray absorption spectroscopy (XAS), X-ray emission spectroscopy (XES), and XPS) in order to identify the differences in an atom specific way. We show that valence electronic structures of these films differ from the bulk and the major factor that separates CoO from FeO is the additional valence electron on Co.

Experimental

The experiments were performed at the elliptically polarized undulator (EPU) beamline 13-2 at Stanford Synchrotron Radiation Lightsource (SSRL). The ultra-high vacuum (UHV) endstation with a base pressure better than 2×10^{-10} Torr is equipped with an electron energy spectrometer (Scienta R3000), high throughput slit-less X-ray emission spectrometer, LEED optics (SPECS), e-beam evaporator (EFM 3, Omicron), and standard tools for sample cleaning. X-ray emission spectrometer is a home-built grazing incidence grating spectrometer with a multichannel-plate detector. A nickel-coated spherical-elliptical grating with 1100 lines/mm groove density was used. The curvature of the grating was 5 m and the length was 10 cm giving an energy resolution of 0.6eV. Sample heating was performed by a standard electron bombardment method, by accelerating electrons emitted from a filament placed backside of the sample. Temperature was measured by a K-type thermocouple spot-welded onto the side of the sample.

Pt(111) single crystal was cleaned by repeated cycles of Ne^+ ion bombardment and annealing to 1150 K. Segregated carbon impurities were burned off by exposing the surface to O_2 while cooling down (from 800 K to 400 K). Long range order and surface cleanness were confirmed by the hexagonal (1×1) sharp LEED patterns and XPS, respectively. FeO and CoO films were prepared by depositing Fe and Co metals using an e-beam evaporator at room temperature and subsequent annealing in 1×10^{-6} Torr O_2 for one minute. Annealing was performed at 950 K in the FeO case, at 840 K for CoO. Background O_2 was pumped out as the

sample temperature went below 400 K. During metal deposition the sample was positively biased in order to prevent sputtering by small amount of ionized metal atoms. Deposition rate was controlled by monitoring the ion flux. Due to two dimensional growth nature of the films, the film completeness could be confirmed by titrating uncovered regions of Pt(111) surface by adsorbed CO. No CO adsorption was observed on both oxide surfaces at room temperature. Gases were dosed into the system by variable leak valves.

The electron binding energies reported here are referenced to the Fermi level of Pt(111). O K-edge XAS spectra were obtained by Auger electron yield method (AEY). Spectra were recorded by placing the kinetic energy window of the spectrometer on the O KVV Auger transition line. Fe and Co L-edge XAS measurements were performed similarly, using energy window of LMM Auger transition. In-plane and out of plane valence orbital components for O $1s{\rightarrow}2p$ and Fe-Co $2p{\rightarrow}3d$ excitations were probed by rotating the sample with respect to polarization $\mathbf{E}$ vector of the synchrotron radiation light. All XAS spectra were normalized to the incident photon flux and background from pure Pt(111) was subtracted. O K-edge XES spectra were recorded by adjusting the grazing incidence angle on the grating to 5°. The excitation energy was set to the first absorption resonance as determined by XAS. In O K-edge XE process the $\mathbf{E}$ vector of the emitted light is aligned with the O $2p$-projected valence orbital. Emission from O $2p_x+2p_y$ and $2p_x+2p_y+2p_z$ orbitals were achieved by recording in XES in normal and grazing emission geometry, respectively[28]. In all XPS, XAS, and XES measurements the grazing incidence angle of the incoming synchrotron light was 4°.

Results

LEED patterns obtained from FeO and CoO bilayers are shown in Fig. 1(a). The analysis of the hexagonal diffraction spots gives rise to Fe-O and Co-O in-plane lattice parameters, 3.08 Å and 3.13 Å, respectively; similar to the ones obtained in previous studies[18,23]. As better visualized on the model drawing of these systems in Fig. 1(a), Moiré superstructure is also well-reproduced, 11 and 13 % planar and 0.6° rotational lattice mismatch with Pt(111) give rise to the Moiré periodicity of 26.3 Å in the FeO case, which is slightly shorter in the CoO case (23.9 Å).

TM $2p$ XPS spectra from FeO and CoO shown in Fig. 1(b) are characterized by spin-orbit splitting into $2p_{1/2}$ and $2p_{3/2}$ components, the energy difference between which increases from 13.4 to 15.7 eV with increasing atomic number. The interference of the satellite components with the main lines complicates the spectral analysis of many $3d$ transition metal oxides[9], however the

sharpness of Co $2p_{3/2}$ main line component is pronounced. The main component of Fe $2p_{3/2}$ located at 709.2 eV is followed by two higher binding energy (BE) components, separated from the main line by 3.0 and 8.7 eV, respectively. Similarly, the sharp main line of the Co $2p_{3/2}$ spectrum at 778.2 eV is broadened by a high BE shoulder centered at 3.2 eV and a higher BE third component is also seen at 8.0 eV. The BE of O $1s$ line of FeO is found to be higher than that of CoO as shown in Fig. 1(c). O $1s$ XPS spectrum of FeO has a main component at 529.4 eV with an asymmetric tail at low BE side. Full width half maximum (FWHM) is 0.9 eV. More asymmetry is observed in CoO, here FWHM is found to be 1.15 eV with the main line centered at 528.9 eV.

VB XPS spectra of FeO and CoO including pure Pt(111) surface are shown in Fig. 2. The measurements were performed by setting the excitation energy close to the Cooper minimum (~hν=200 eV) of Pt $5d$ states[29] so that their contribution to the overall VB spectra is minimized. The combination of normal and grazing detection geometry along with low kinetic energy additionally provides identification of oxide related spectral features, which overlap with Pt $5d$ states of the underlying Pt substrate. In normal geometry, distinct spectral features from O $2p$ and Fe-Co $3d$ are observed however in grazing geometry the substrate contribution is nearly vanished. Both FeO and CoO VB contain three distinguishable spectral features, one of which is in close proximity to the Fermi edge. The intensity of this peak is rather pronounced in CoO. The second clearly identifiable peak resides at 5.3 eV in FeO and 4.9 eV in CoO. The region between these two can be realized by a third component. In the case of FeO, the peak at 3.4 eV seems to be sharper as compared to CoO. Nevertheless, a peak centered at 2.1 eV is seen in CoO. The intensity analysis[30] performed by including the ionization cross-sections,[29] electron inelastic mean free paths[31], and electron emission geometry reveals that, in grazing geometry, the TM $3d$ contribution dominates the VB spectra. For FeO and CoO films the TM $3d$/Pt $5d$ intensity ratios are estimated to be 16.2 and 21.6, respectively. The contribution of O $2p$ states is less pronounced, but should be detectable.

VB spectra shown in Fig. 2 involve information regarding the electronic properties of these films; however overlapping TM $3d$ and O $2p$ states makes the spectral characterization nontrivial. The atom specific approach to probe electronic structure of these films is to take advantage of the dipole transitions; $1s{\rightarrow}2p$ and $2p{\rightarrow}1s$ in the case of O K-edge absorption and emission measurements, respectively. Occupied and unoccupied p-states projected on oxygen

6

atoms of these films can then be identified. $2p_x+2p_y$ and $2p_z$ symmetry resolved XES and XAS spectra from FeO and CoO films are shown in Fig. 3. Spectra were aligned with respect to each other in BE scale so that a direct comparison can be made[32]. The Fermi edge is determined by using peak maxima of O $1s$ XPS spectra from respective films[28]. Certain differences in spectral weights are apparent. XAS shows states above the Fermi level, a clear signature of covalent interaction of TM-O bonding complex. Another important finding to note here, unlike bulk oxide electronic structures, FeO and CoO films on Pt(111) surfaces have states tailing near the Fermi level. Main bonding components of O $2p_x+2p_y$ and O $2p_z$ states are at 5.6-4.1 eV and 5.1-4.0 eV below the Fermi level for FeO and CoO films, respectively. All spectra have low BE shoulder spanning up to the Fermi level. Spectral weights of the shoulders of the O $2p_z$ states are more pronounced, and CoO seems to have more states near the Fermi level compared to FeO. First sharp state with anti-bonding character above the Fermi level is attributed to O $2p$-TM $3d$ hybridized states. FeO has intrinsically sharper peaks and the energy difference between resonant maxima of $2p_x+2p_y$ and $2p_z$ is 0.4 eV. This difference becomes 0.3 eV in CoO, $2p_z$ of which is also closer to the Fermi level. The energy window covering 4-16 eV above the Fermi level is dominated by O $2p$-TM $4sp$ hybridized states; a clear distinction is that $2p_x+2p_y$ components are more intense as compared to $2p_z$. The main peak of FeO is at 10.5 eV, that of CoO is at slightly lower energy. Nevertheless; the broad widths of these peaks make the direct comparison difficult.

TM L-edge XAS spectra of these films are relatively less complex due to single cation valence structure. Fig. 4 shows the Fe-Co L-edge XAS spectra for respective oxide films with in plane and out of plane **E** vector to the projected TM $3d$ component. On the L_3 edge, CoO spectra width is relatively narrower compared to FeO, which has a prominent shoulder tailing low energy side. This pre-edge component is almost absent in CoO. In both films, L_3 edge can also be interpreted as a main peak with a shoulder on high photon energy side. On the L_2 edge, peaks are broad and featureless however spectral width comparison reveals a sharper Co L_2 edge. No strong polarization dependence is observed.

Discussion

One of mutual structural properties of these films is the oxygen termination. Previous studies indicate that the main characteristic is the out of plane TM-O interatomic distance; that is approximately 50 % shorter relative to the bulk values. There are also other differences, the

7

electronic structures of these FeO and CoO films grown on Pt(111) surfaces can be separated from each other by the valence electronic properties of the TMs, Co having an additional valence electron than Fe. The Moiré periodicity of FeO is slightly longer but the differences in the in-plane metal-oxygen bond lengths are too small, thus have a little impact on the overall electronic structure. The registry with the Pt(111) substrate, however, slightly modifies out of plane TM-O bond length. Interfacial metal atoms can be found on three-fold fcc, hcp, and top sites of Pt(111) surface and their effects are translated into Moiré superstructure observed on these films[33]. It has been shown by STM studies that the surface potential of FeO films becomes modulated due to corrugation of the Moiré superstructures[20,34]. Despite the lack of information that quantifies the variation of the surface potential of CoO films, a similar behavior is expected.

For bulk FeO and CoO, the charge transfer energy is moderate ($W/2 < \Delta < U_{dd}$)[9] and O $2p$ valence states overlaps with the TM $3d$ states. It is therefore important to separate out the TM and ligand states in order to make electronic structure comparisons viable. We have shown that O K-edge XES selectively probes O $2p$ states and their contribution to the overall valence structure can be singled out by VB XPS. In the case of thin films a modified picture must be considered; valence states of the films will be overlapping with those of Pt.

These parameters can be approximated by the analysis of CL and VB XPS spectra. The satellite features observed in $2p$ XPS spectra of the late TM monoxide compounds have been attributed to charge transfer mechanism, from the ligand to the metal site, and to the multiplet effects[35], however this approach has been challenged since it neglects the angular momentum coupling of the TM $3d$ electrons and ionized core levels[36]. The late $3d$ TM monoxides have shown complex behavior to sudden creation of a core hole, suggesting differences in their VB structures. The final state of the photoemission process contains core hole which is coupled with the partially filled TM $3d$ states, giving rise to mainline broadening and satellite features in XPS spectra depending on the particular overlap between core levels and the valence states. These multiplet effects are represented by U_{cd}, c being the core hole states (the change in the VB electronic configuration is alternatively illustrated by Z+1 approximation, where Z is the atomic number)[37,38]. The extent of the spatial interaction between orbitals can directly be reflected to the XPS spectra. Resonant and non-resonant photoemission studies have also shown $3s3p$-$3d$ overlap which leads to the satellites and resonant enhancements; however multiplet effects can be translated as spectral broadening in TM $2p$ XPS spectra due to smaller overlap between $2p$ hole

and $3d$ orbitals[39]. It must therefore be noted here that the analysis of CL $2p$ spectra does not directly provide U_{dd} and Δ parameters which can be better described in ground state electronic structures. When a $2p$ core hole is created, two final state electronic configurations are described by cd^n and $cd^{n+1}\underline{L}$, and the energy difference between these two final states, U_{cd}-Δ, determines the BE of the satellite peaks. The satellites of the TM $2p$ XPS spectra presented in Fig. 1(b) indicate similar mechanism, involvement of at least two different final states. Another point to note is the relative intensities, the satellite features of FeO seem to have more pronounced intensity (although smeared out) compared to the main well-screened line. These differences are attributed to the screening efficiency of the metallic substrate. Efficiency of the hole screening is evidenced by the sharpness of Co $2p$ XPS peaks, also suggesting metallic behavior. In addition, BE of Co $2p_{3/2}$ main line peak position appears to be slightly lower than BE of Co^{2+} of the bulk systems[9]. Despite the differences in the intensity ratios of the main lines to the satellite peaks, c(4×2) and (9×2) phases of the cobalt oxides grown on Pd(100) demonstrate similar BEs[40]. XPS spectrum of FeO films is identical to the previously published data[21].

2p XPS spectra of FeO and CoO show two peaks separated by U_{cd}-Δ, the energy difference between unscreened and well-screened cd^6 and $cd^7\underline{L}$ final states in FeO, and the difference between cd^7 and $cd^8\underline{L}$ final states in CoO. The shoulders residing ~3 eV high BE side of the well-screened main lines are attributed to the multiplet effects which are stronger in $2p_{3/2}$ states than $2p_{1/2}$[41]. Comparing the relative intensities and the energy differences between main and satellite peaks presented in Fig. 1(b) with the previously reported spectra from bulk samples, one can notice certain differences[39,42]. The satellites of the thin films seem to be less pronounced and U_{cd}-Δ values are relatively larger. It is worthwhile to point out that structure mediated hybridization shifts are also involved in the energy separation. It has been reported that U_{cd}-Δ obtained from $2p$ XPS spectra of bulk FeO and CoO is 6.04 and 5.8 eV, lower than the energy differences that thin films display (8.7 and 8.0 eV). This would suggest that U and Δ are modified for the thin films due to their image dipoles on metal substrates.

Electronic and magnetic properties of the late TM oxides grown on metal substrates differ since the Coulomb and charge transfer energies in thin films have smaller values due to efficient image potential screening[43]. The reduction in Δ has been proposed to be the main contributor to the larger energy separation between the main and the satellite peaks (U_{cd}-Δ), mainly in connection to the possibly lower Madelung potential. U_{cd} remains larger than the d-

band width w despite orbital overlap with the substrate and the effect of the core hole can be assumed to be unchanged since screening takes place from the VB of the same atom. The intensities of the satellite peaks are also expected to be more pronounced under the circumstances where Δ is reduced (in the presence of the core hole)[44]. The origin of the discrepancy of the ratio of satellite to main peaks between the thin films and the bulk samples is the effect of the hybridization strength[45] between TM $3d$ and O $2p$ states, which is enhanced due to the shorter out of plane TM-O bond lengths and also due to the lateral strain in the film (the influence of the latter is expected to be weaker since the bond lengths of the former is more modified). The hybridization effect is also evident from the VB XPS and XES spectra, energies of O $2p$ and TM $3d$ states significantly overlap in the range below the Fermi level. Larger peak difference in FeO compared to bulk could thus reflect the different Fe-O bond lengths. Moreover, the contribution of the Pt $5d$-TM $3d$/O $2p$ spatial overlap is not insignificant, as it will be discussed below in the analysis of the VB structures.

The effect of the screening manifests itself in O $1s$ XPS spectra shown in Fig. 1(c). O $1s$ BE of CoO is found to be 0.5 eV lower than that of FeO which has not been the case for bulk monoxides. Lower O $1s$ BE has been observed in MnO, but FeO, CoO, and NiO have O $1s$ XPS spectra with rather similar binding energies[42]. This situation is unique for monolayer thin oxide films grown on metallic substrates, where increasing the layer thicknesses the electronic properties converge to the bulk behavior, thus XPS spectra of the films thicker than 5 atomic layers are expected to become identical to the bulk[46,47]. The energy of the oxygen ligand at the final state determines the O $1s$ BE, which are different in these two situations, and the evidence to difference is the O $2p$ electronic structure presented in O K-edge XES spectra. Although LEED pattern shows perfect long range order, CoO films could be slightly more defective at the atomic scale and it might give rise to the larger FWHM. However, the presence of the other species such as hydroxyl groups (–OH) must be ruled out since no XES-XAS spectral features that could point to their existence have been observed.

Charge transfer energy Δ can be approximated as the electron-hole pair excitation between the lowest unoccupied and the highest occupied states in the O $2p$-TM $3d$ hybridized system. This can be obtained from O K-edge XES and XAS spectra by taking the energy difference between the lowest unoccupied and the highest occupied states. The highest lying occupied O $2p$ state can be directly obtained, however one needs to assume that O $2p$-TM $3d$

hybridized state in the absorption spectra determines the lowest unoccupied state of the metal site. Another important caution that one needs to take into account is the final state effects in X-ray absorption and emission processes. In the absorption event the final state has an O $1s$ core hole whereas the core hole is filled in the emission event. Presence of the core hole in the final state generally shifts XAS spectra to lower BE and excitonic effects could potentially modify the intensity of XAS peaks[48]. Therefore, approximated Δ values are probably lower than the values reported in the literature and in present work. Nevertheless, following this approach the change in Δ in bulk samples has been found to be in the order along which the systems become more ionic: NiO<CoO<MnO; 5.4, 6.1, and 6.6 eV, respectively[8]. The examination of electronic structure shown in Fig. 3 reveals that the energy separation between the oxygen bonding and the antibonding states are much smaller compared to the bulk samples; 2.2 eV (FeO) and 1.6 eV (CoO) are the approximated Δ values of bilayer films. More importantly, density of states (DOS) near the Fermi level is non-vanishing, further suggesting a deviation from the bulk electronic structures. Larger Δ values with decreasing atomic number of $3d$ TM are consistent with the trend in the bulk TM monoxides[8,39]. This indicates that image dipole and hybridization causes reduction in Δ; the trend among $3d$ TM monoxide films is persistent provided that they are isostructural.

The distribution of O $2p$ and TM $3d$ DOS over the occupied part of the band structure can be identified by comparison of VB XPS (Fig. 2) with O K-edge XES (Fig. 3). The XES spectral signatures arise from hybridized TM-O chemical bond resulting in a bonding and antibonding orbitals of oxygen atoms. In bulk FeO and CoO, TM cations have the octahedral symmetry, surrounded by six oxygen anions. In this configuration TM $3d$ orbital split into two bond configurations: σ (e$_g$: $d_{x^2-y^2}$, d_{z^2}) and π (t$_{2g}$: d_{xy}, d_{xz}, d_{yz}), where the TM-O hybridization strength differs due to bond anisotropy. The energy differences between these two levels depend on the number of d electrons in the ground state and also TM-O chemical bond length. The orbital overlap on (111) plane of the thin films will have a similar interpretation. The interactions on the (111) plane induce a stronger overlap between the O $2p$ and TM $3d$ orbitals. One can also view this system as a monolayer of oxygen atoms bound to the three-fold sites of monolayer TM film. In an fcc-hollow site, O $2p_x$-$2p_y$ orbitals are involved more in the chemical bonding, where the largest orbital overlap with TM $3d$ orbitals occurs through the σ interaction between TM 3d ($d_{x^2-y^2}$, d_{xy}) and O $2p$ orbitals. Whereas perpendicular to the (111) plane the π bonding interaction

11

between O $2p_z$ and TM $3d$ (d_{xz}, d_{yz}, d_{z^2}) orbitals is realized[49]. Larger overlap for σ interaction in the (111) plane translate to a larger energy separation between bonding and antibonding states as observed in the XES and XAS spectra. The bond strength of TM-O can thus be estimated by comparing the energy difference, the stronger Fe-O interaction gives rise to an energy separation (6.9 eV), larger than Co-O (6.0 eV). As in both cases O $2p$ states spills over the Fermi level.

The broad peaks covering 5-8 eV energy range in VB spectra in grazing geometry shown in Fig. 2 are straightforwardly assigned to O $2p$ states but the region below 5 eV is more difficult to interpret due to the mixed TM $3d$-O $2p$ states. VB spectra qualitatively agree with the previous studies[21,40,50,51], in the present work the spectral features are much better resolved. Pt $5d$ states still contribute to the spectra taken in normal electron emission geometry whereas they nearly vanish in grazing geometry. As in XES spectra, O $2p$ derived states in FeO (5.3 eV) shifts to lower BE in CoO (4.9 eV). Previous resonant photoemission studies at the TM $3p\rightarrow3d$ absorption threshold identified the resonant enhancements of $3d$ derived states in VB XPS spectra[50,51]. In the light of these studies, the sharp peak just 1 eV below the Fermi edge, broad peaks covering 1-4 eV and 8-14 eV energy region are assigned to TM $3d$ states, the former with strongly hybridized characteristics. The peak at ~1 eV is assigned to well screened $d^n\underline{L}$ (n=6, 7 in FeO and CoO) level at the final state. Apparent intensity domination of this peak in CoO also puts forwards the effect of the hybridization with the oxygen states, an observation in line with XES spectra. The rather broad peaks ~10.8 eV (FeO) and 10.2 eV (CoO) below the Fermi edge are attributed to d^{n-1} final states. Despite their weak intensity observed here, their existence as a photoionized final state has been justified by the resonant and angle resolved photoemission studies [50–52]. The energy difference between these high BE peaks and the first TM $3d$ absorption resonance peak above the Fermi level (presumably at the same energy as the first resonance in O XAS) corresponds to U_{dd} and it is certainly higher than 11 eV. This value is in the range of Coulomb energies estimated and calculated for late TM monoxides[51] and also quite larger than charge transfer energies. This result indicates that our initial assumption of U being unchanged due to image charge screening is reasonable.

O K-edge and TM L-edge XAS spectra presented in Fig. 3 and Fig. 4 highlight the anisotropy of the hybridization between orbitals. First resonant feature is larger in width compared to the pure metal L-edge spectra[53] but π^* and σ^* antibonding states are not seen clearly. This indicates that the crystal field is not as strong as in the case of bulk TM monoxides.

FWHM of the first resonance peaks in FeO seems to be larger suggesting that the energy difference between σ^* and π^* orbitals is larger. This is indeed confirmed by O K-edge XAS, the first resonance in $2p_x+2p_y$ symmetry resides 0.3 eV higher energy than the one in $2p_z$. $2p$-$4sp$ hybridized peak at ~10 eV above the Fermi edge is more intense in FeO and thereby the bonding interaction on (111) plane is stronger.

Symmetry resolved intensity differences in XAS spectra also reveal that TM-O bond geometry is more anisotropic in CoO. This comparison is basically based on the similar bulk lattice parameters, on an ideal monoxide structure where TM is octahedrally coordinated to the oxygen anions. It can be attributed to the lateral strain, as a consequence that the Co-O lattice is extended more out of plane. The anisotropy in the bond symmetry can also be attributed to more pronounced O $2p$ states right below the Fermi level as shown by XES. Nevertheless, both films show structural resemblance but their electronic properties are slightly different with respect to each other.

Conclusions

Core level spectroscopy has been utilized to characterize the electronic properties of polar FeO and CoO single TM-O bilayer-thick, isostructural films grown on Pt(111). The differences in the core level spectral features of these films scale well with the spectra obtained from bulk samples, but deviations between the TM monoxides of the same metals are related to the screening and bonding properties of substrate metal. In addition, TM-O interatomic distances contribute to the modified electronic structures of the FeO and CoO films and consequently their influence is reflected in the core level spectral features. Oxygen density of states below and above the Fermi level and overall valence band electronic structure give evidences that electronic states of these films are strongly coupled with the Pt substrate states. The conclusions drawn here may potentially play an important role in understanding magnetic, electronic, and surface chemical properties of TM monoxides on metallic substrates. These oxides are also active towards certain surface chemical reactions, such as oxygen evolution reaction of importance in water splitting and Fischer-Tropsch process for synthesis of hydrocarbons, modified bond lengths imply that these thins films are involved in oxidation reduction surface chemical cycles in different ways.

Acknowledgements

References

[1] D. Cappus, M. Hassel, E. Neuhaus, M. Heber, F. Rohr, and H.J. Freund, Surf. Sci. **337**, 268 (1995).

[2] P W Tasker, J. Phys. C Solid State **12**, 4977 (1979).

[3] J. Goniakowski, F. Finocchi, and C. Noguera, Rep. Prog. Phys. **71**, 016501 (2008).

[4] J. Goniakowski, C. Noguera, and L. Giordano, Phys. Rev. Lett. **98**, 205701 (2007).

[5] J. Zaanen, G.A. Sawatzky, and J.W. Allen, Phys. Rev. Lett. **55**, 418 (1985).

[6] K. Terakura, T. Oguchi, A.R. Williams, and J. Kübler, Phys. Rev. B **30**, 4734 (1984).

[7] K.C. Prince, M. Matteucci, K. Kuepper, S.G. Chiuzbaian, S. Bartkowski, and M. Neumann, Phys. Rev. B **71**, 085102 (2005).

[8] E.Z. Kurmaev, R.G. Wilks, A. Moewes, L.D. Finkelstein, S.N. Shamin, and J. Kuneš, Phys. Rev. B **77**, 165127 (2008).

[9] G. Lee and S.-J. Oh, Phys. Rev. B **43**, 14674 (1991).

[10] H.-J. Freund and D.W. Goodman, in *Handbook of Heterogeneous Catalysis* (Wiley-VCH Verlag GmbH & Co. KGaA, 2008).

[11] Q. Fu, W.-X. Li, Y. Yao, H. Liu, H.-Y. Su, D. Ma, X.-K. Gu, L. Chen, Z. Wang, H. Zhang, B. Wang, and X. Bao, Science **328**, 1141 (2010).

[12] J.S. Corneille, J.-W. He, and D.W. Goodman, Surf. Sci. **338**, 211 (1995).

[13] K. Mori, M. Yamazaki, T. Hiraki, H. Matsuyama, and K. Koike, Phys. Rev. B **72**, 6 (2005).

[14] E. Yagasaki and K. Kishi, J. Electron. Spectrosc. **69**, 133 (1994).

[15] M. Hassel and H.-J. Freund, Surf. Sci. **325**, 163 (1995).

[16] S. Sindhu, M. Heiler, K.-M. Schindler, and H. Neddermeyer, Surf. Sci. **541**, 197 (2003).

[17] C. Giovanardi, L. Hammer, and K. Heinz, Phys. Rev. B **74**, 125429 (2006).

[18] Y.J. Kim, C. Westphal, R.X. Ynzunza, H.C. Galloway, M. Salmeron, M.A. Van Hove, and C.S. Fadley, Phys. Rev. B **55**, 13448 (1997).

[19] M. Ritter, W. Ranke, and W. Weiss, Phys. Rev. B **57**, 7240 (1998).

[20] L. Giordano, G. Pacchioni, J. Goniakowski, N. Nilius, E.D.L. Rienks, and H.J. Freund, Phys. Rev. B **76**, 075416 (2007).

[21] T. Schedel-Niedrig, W. Weiss, and R. Schlogl, Phys. Rev. B **52**, 17449 (1995).

[22] Y. Yao, Q. Fu, Z. Wang, D. Tan, and X. Bao, J. Phys. Chem. C **114**, 17069 (2010).

[23] M. De Santis, A. Buchsbaum, P. Varga, and M. Schmid, Phys. Rev. B **84**, 125430 (2011).

[24] S. Entani, M. Kiguchi, and K. Saiki, Surf. Sci. **566-568**, 165 (2004).

[25] B. Hammer and J.K. Norskov, in *Impact of Surface Science on Catalysis* (Academic Press, 2000), pp. 71–129.

[26] A. Nilsson, L.G.M. Pettersson, B. Hammer, T. Bligaard, C.H. Christensen, and J.K. Nørskov, Catalysis Letters **100**, 111 (2005).

[27] C. Noguera, J. Phys. Condens. Mat. **12**, R367 (2000).

[28] A. Nilsson and L.G.M. Pettersson, Surf. Sci. Rep. **55**, 49 (2004).

[29] J.J. Yeh and I. Lindau, Atom. Data Nucl. Data Tables **32**, 1 (1985).

[30] The contributions of Pt $5d$, TM $3d$, and O $2p$ states to the VB XPS spectra could be estimated by spectral intensity calculations taking into account ionization cross-sections (σ), inelastic mean free path of the electrons (λ), and electron emission detection geometry (θ). The intensity ratio of the spectral contribution of the films to the spectral contribution from the Pt(111) substrates is given by: $I_{film}/I_{Pt(111)}=(\sigma_{film}/\sigma_{Pt(111)})exp(d/\lambda sin\theta)$, where d is the thickness of the FeO and CoO films. Theoretically estimated ionization cross-sections at hv=165 eV[29] favor contributions from the films over the substrate; 14.2, 18.8, and 2.4 Correspond to $\sigma_{film}/\sigma_{Pt(111)}$ obtained from (TM $3d$/Pt $5d$) and (O $2p$/Pt $5d$) of FeO and CoO films, respectively. As a first approximation the thickness of the films can be assumed to be similar and d therefore can be taken as 0.80 Å[33].

Includingλ though FeO and CoO, 6.09 Å and 5.75 Å[31], respectively; 12.3:16.1:1 is obtained for $3d/5d$ intensity fraction of FeO:CoO:Pt in normal emission geometry and the enhancement in grazing geometry is found to be 16.2:21.6:1. The contribution of O $2p$ spectra is smaller, $2p/5d$ intensity fraction of FeO:CoO:Pt in normal and grazing geometries are 2.07:2.05:1 and 2.74:2.76:1, respectively. The contribution of Pt $6s$ states to the VB spectra was disregarded since the ionization cross section at 165 eV is smaller than order of magnitude[29].

[31] S. Tanuma, C.J. Powell, and D.R. Penn, Surf. Interface Anal. **20**, 77 (1993).

[32] A. Nilsson, J. Electron. Spectrosc. **126**, 3 (2002).

[33] W.H. Zhang, Z.Y. Li, Y. Luo, and J.L. Yang, J. Phys. Chem. C **113**, 8302 (2009).

[34] E.D.L. Rienks, N. Nilius, H.P. Rust, and H.J. Freund, Phys. Rev. B **71**, 241404 (2005).

[35] G. van der Laan, C. Westra, C. Haas, and G.A. Sawatzky, Phys. Rev. B **23**, 4369 (1981).

[36] P.S. Bagus, R. Broer, W.A. de Jong, W.C. Nieuwpoort, F. Parmigiani, and L. Sangaletti, Phys. Rev. Lett. **84**, 2259 (2000).

[37] S. Hüfner, *Photoelectron Spectroscopy* (Springer, Berlin, 2003).

[38] F. de Groot and A. Kotani, *Core Level Spectroscopy of Solids* (CRC Press, Boca Raton, FL, 2008).

[39] R. Zimmermann, P. Steiner, R. Claessen, F. Reinert, S. Hufner, P. Blaha, and P. Dufek, J. Phys. Condens. Mat. **11**, 1657 (1999).

[40] L. Gragnaniello, S. Agnoli, G. Parteder, A. Barolo, F. Bondino, F. Allegretti, S. Surnev, G. Granozzi, and F.P. Netzer, Surf. Sci. **604**, 2002 (2010).

[41] K. Okada and A. Kotani, J. Phys. Soc. Jpn. **61**, 4619 (1992).

[42] F. Parmigiani and L. Sangaletti, J. Electron. Spectrosc. **98-99**, 287 (1999).

[43] S. Altieri, L.. Tjeng, and G.. Sawatzky, Thin Solid Films **400**, 9 (2001).

[44] J. Zaanen, C. Westra, and G.A. Sawatzky, Phys. Rev. B **33**, 8060 (1986).

[45] A.E. Bocquet and A. Fujimori, J. Electron. Spectrosc. **82**, 87 (1996).

[46] S. Altieri, L.H. Tjeng, F.C. Voogt, T. Hibma, and G.A. Sawatzky, Phys. Rev. B **59**, R2517 (1999).

[47] S.A. Chambers and T. Droubay, Phys. Rev. B **64**, 075410 (2001).

[48] P.A. Brühwiler, A.J. Maxwell, C. Puglia, A. Nilsson, S. Andersson, and N. Mårtensson, Phys. Rev. Lett. **74**, 614 (1995).

[49] T. Wiell, J.E. Klepeis, P. Bennich, O. Björneholm, N. Wassdahl, and A. Nilsson, Phys. Rev. B **58**, 1655 (1998).

[50] R.J. Lad and V.E. Henrich, Phys. Rev. B **39**, 13478 (1989).

[51] Z.-X. Shen, J.W. Allen, P.A.P. Lindberg, D.S. Dessau, B.O. Wells, A. Borg, W. Ellis, J.S. Kang, S.-J. Oh, I. Lindau, and W.E. Spicer, Phys. Rev. B **42**, 1817 (1990).

[52] S. Masuda, Y. Harada, H. Kato, K. Yagi, T. Komeda, T. Miyano, M. Onchi, and Y. Sakisaka, Phys. Rev. B **37**, 8088 (1988).

[53] H.-J. Kim, J.-H. Park, and E. Vescovo, Phys. Rev. B **61**, 15284 (2000).

List of figures

Figure 1. (a) LEED pattern and structural model of FeO and CoO films grown on Pt(111). Patterns were obtained by setting the kinetic energy of the incident electrons to 95 eV. (b) Co and Fe $2p$ XPS spectra recorded using photon energy hν=880 eV and hν=940 eV, respectively. (c) O $1s$ XPS spectra of respective films. They are both recorded using the same photon energy, hν=700 eV. Red and blue represent pattern/atom/spectrum of FeO and CoO, respectively.

Figure 2. Valence band XPS spectra of FeO (red), CoO (blue) and pure Pt(111) (black) recorded at a photon energy hν=165 eV. Normal emission spectra (dotted) labeled separately from grazing emission spectra (solid) which was measured by setting electron take-off angle to 79° from the surface normal. Final states are denoted on the respective spectra.

Figure 3. O K-edge absorption and emission spectra obtained from FeO and CoO films. The spectra were aligned in the BE scale using O $1s$ XPS presented in Fig. 1(c). Spectra representing $2p_x+2p_y$ (normal), $2p_z$ (grazing) symmetry components are shown as solid and dotted lines, respectively.

Figure 4. Fe and Co L-edge XAS spectra obtained from FeO and CoO films. They were recorded in two geometries and shown spectra represent unoccupied $3d$ states hybridized with O $2p_x+2p_y$ (normal) and O $2p_z$ (grazing) states.
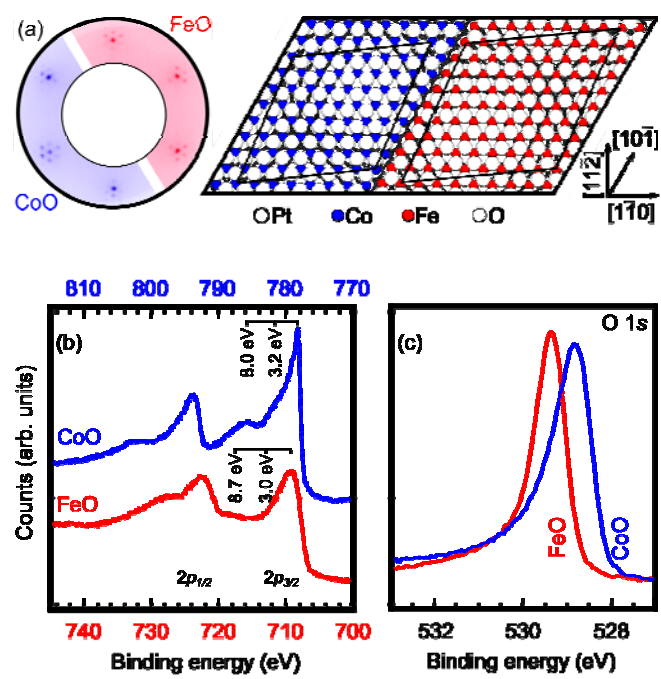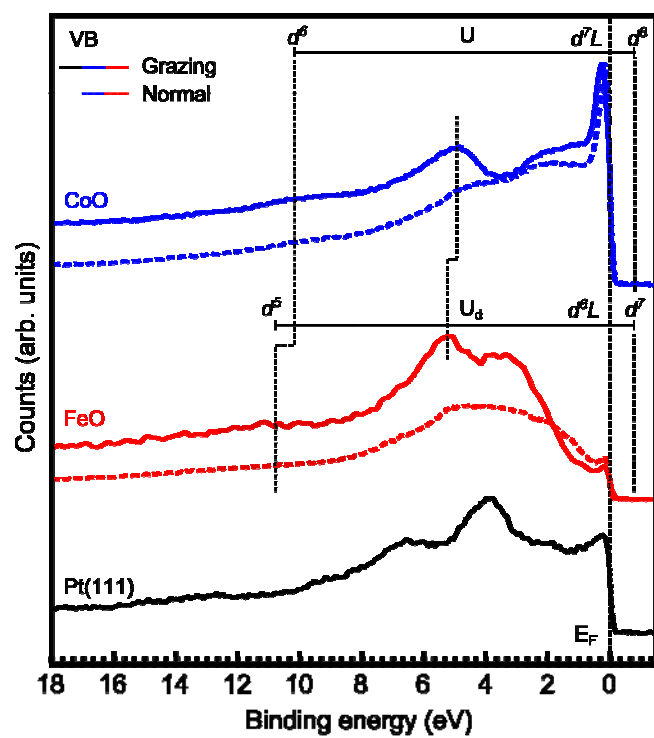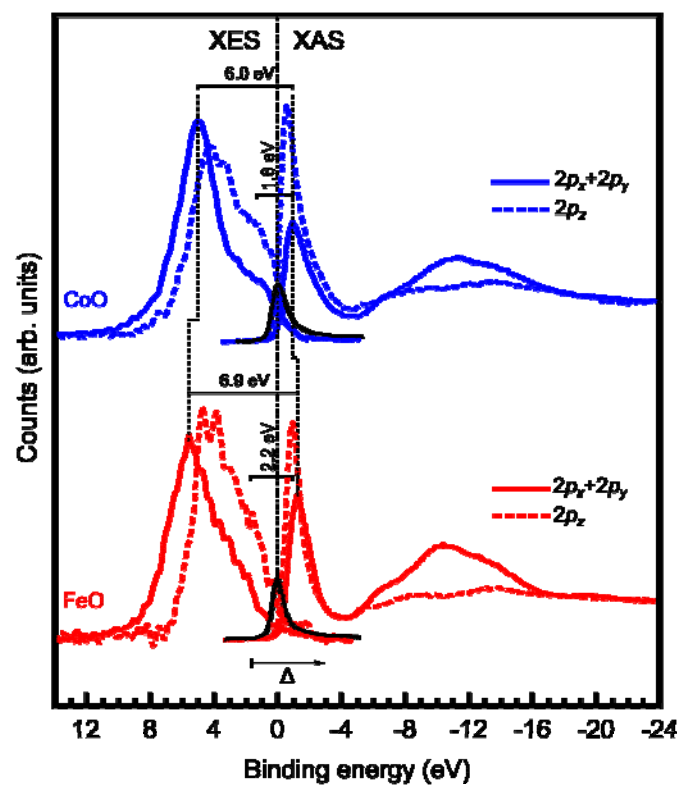
Figure 1

Figure 2

Figure 3

Figure 4